



**RESEARCH ARTICLE**

**OPTIMIZATION OF T6 HEAT-TREATED Al<sub>2</sub>O<sub>3</sub>-CNT REINFORCED ALUMINIUM COMPOSITE: MICROSTRUCTURAL AND MECHANICAL PROPERTIES ANALYSIS**

**Mohammad Na'aim Abd Rahim<sup>1</sup>, Mohd Shukor Salleh<sup>1,\*</sup>, Nur Farah Bazilah Wakhi Anuar<sup>1</sup>, Saifudin Hafiz Yahaya<sup>1</sup>, Salah Salman Al-Zubaidi<sup>2</sup>**

<sup>1</sup>*Fakulti Teknologi Dan Kejuruteraan Industri Dan Pembuatan, Universiti Teknikal Malaysia Melaka, Hang Tuah Jaya, 76100, Durian Tunggal, Melaka, Malaysia.*

<sup>2</sup>*Department of Automated Manufacturing Engineering, Al-Khwarizmi College of Engineering, University of Baghdad, 10071 Baghdad, Iraq.*

**Abstract.** Metal matrix composites (MMCs) are widely used because of their high strength-to-weight ratios, excellent wear resistance, and thermal conductivity. Numerous studies have explored optimizing the mechanical properties of MMCs using hybrid nanoparticle reinforcements. In this study, alumina (Al<sub>2</sub>O<sub>3</sub>) and carbon nanotubes (CNTs) were used to reinforce aluminium alloy A356 through electromagnetic stirring (EMS), followed by T6 heat treatment. The composite fabrication involved varying Al<sub>2</sub>O<sub>3</sub>-CNT compositions and stirring durations. Optimization was conducted using the Taguchi Method to obtain the optimum combination of Al<sub>2</sub>O<sub>3</sub>-CNT. The influence of hybrid reinforcements and EMS on the microstructural distribution and mechanical properties was analyzed. Optical microscopy (OM) revealed that Al<sub>2</sub>O<sub>3</sub>-CNT reinforcement refined the grains and caused notable changes from dendritic to rosette structures, leading to closely packed grains with reduced porosity. Intermetallic phases in the composite were characterized using Field Emission Scanning Electron Microscopy (FESEM) and X-ray Diffraction (XRD). The results revealed that the composite with 0.5 wt.% CNTs, 6 wt.% Al<sub>2</sub>O<sub>3</sub>, and 10 minutes of stirring time produced higher mechanical properties compared to other parameters. Under these conditions, yield strength, ultimate tensile strength, and elongation to fracture increased from 94.09 MPa, 221.10 MPa, and 11.37% to 117.18 MPa, 288.08 MPa, and 14.5%, respectively, after T6 heat treatment. These findings suggest that optimized reinforcement parameters, combined with T6 treatment, can significantly enhance the mechanical performance of Al<sub>2</sub>O<sub>3</sub>-CNT hybrid-reinforced aluminium alloys, making them promising materials for high-performance applications.

**Keywords:** Metal matrix composite, CNT-Al<sub>2</sub>O<sub>3</sub> reinforcement, T6 heat treatment, mechanical properties.

**Article Info**

Received 30 December 2024

Accepted 4 March 2024

Published 2 June 2025

**\*Corresponding author: [shukor@utem.edu.my](mailto:shukor@utem.edu.my)**

Copyright Malaysian Journal of Microscopy (2025). All rights reserved.

ISSN: 1823-7010, eISSN: 2600-7444

## 1. INTRODUCTION

Aluminium metal matrix composites (AMCs) are innovative materials extensively employed across multiple industries because of their outstanding lightweight properties, high corrosion resistance, high thermal conductivity, and high strength-to-weight ratio [1]. Currently, aluminium alloys are widely used in the transportation sector for vehicle bodies, engine components and ship propellers. The integration of aluminium into automotive design has yielded benefits such as increased speed, improved safety, enhanced fuel efficiency and reduced emissions [2]. The most commonly used reinforcements include silicon carbide (SiC), aluminium oxide ( $\text{Al}_2\text{O}_3$ ) and titanium boride ( $\text{TiB}_2$ ). These reinforcements enhance the tensile strength, hardness, density and wear resistance of aluminium and its alloys. In recent years, the use of CNTs and  $\text{Al}_2\text{O}_3$  as reinforcements in composites has been widely recognized for their role in enhancing material strength. CNTs are cylindrical molecules comprising carbon atoms arranged in a hexagonal structure, similar to graphite. They possess extraordinary mechanical, electrical and thermal properties, which make them highly valuable in materials science and engineering. For instance, CNTs in aluminium composites contribute to increased mechanical strength without significantly increasing weight. Meanwhile, alumina is a crystalline powder that is highly valued for its hardness, strength and thermal stability [3]. Alumina serves as a reinforcement material in composite materials, helping to improve hardness, wear resistance and overall durability.

Nowadays, researchers have actively explored proper ways to improve the matrix composite through hybrid reinforcement method which employed two or more reinforcement particles into the matrix [4,5]. The primary method used to produce  $\text{Al}_2\text{O}_3$ -CNTs reinforced aluminium matrix composites (AMCs) is powder metallurgy (PM) [6]. Although powder metallurgy enables precise control over composition and near-net-shape fabrication, it remains a time-consuming and multi-step process involving powder production, compaction, and sintering. These stages often introduce issues such as residual porosity, oxygen contamination, and microstructural inhomogeneity, which can compromise the ductility and mechanical integrity of the final. For example, Shan et al. [7] employed powder metallurgy to produce  $\text{Al}_2\text{O}_3$ -CNTs /Al composites. The optimum result of 0.5 wt.% CNTs and 10 wt.% in-situ  $\text{Al}_2\text{O}_3$ , showing a 133% improvement in yield strength (YS) and a 121% increase in ultimate tensile strength (UTS) from the pure aluminium. This enhancement in strength was accompanied by a significant reduction in ductility. To address this issue, multiple steps are necessary, including planetary ball milling, composite powder mixing, cold pressing, sintering, and hot extrusion. While these processes are effective, they also lead to increased costs and fabrication time for the matrix.

On the other hand, electromagnetic stirring (EMS) has emerged as a major advancement in semi-solid processing, offering distinct benefits over traditional methods. EMS offers a single-step, in-situ refinement process that significantly enhances microstructural uniformity by breaking up dendritic structures during solidification, which improves mechanical properties and reduces segregation. This technique not only enhances the quality of cast materials but also improves their mechanical properties, making it highly advantageous for various metal manufacturing applications. One of EMS's key advantages is its precise control over the microstructure of cast materials, as it can enhance the size and distribution of precipitation during melting. Unlike conventional casting, which often yields dendritic structures that may weaken mechanical performance, EMS promotes the formation of non-dendritic, globular microstructures. This refinement is essential, as it enhances mechanical properties like strength and toughness. EMS has demonstrated the capability to eliminate voids and improve particle distribution, thereby producing composites with fewer defects and superior mechanical properties compared to those fabricated via PM [8]. The ability to achieve finer, more consistent microstructures directly enhance the overall performance of the final product.

T6 heat treatment, consisting of solution heat treatment followed by quenching and artificial aging, plays a vital role in enhancing the mechanical performance of metal matrix composites. During solution treatment, alloying elements dissolve into the matrix, creating a supersaturated solid solution. Subsequent aging promotes the controlled precipitation of strengthening phases, such as  $\text{Mg}_2\text{Si}$  in aluminum alloys, which impedes dislocation motion and significantly improves hardness, tensile strength, and fatigue resistance. In composites, the T6 process also helps relieve residual stress

introduced during fabrication and enhances interfacial bonding between the matrix and reinforcement particles. These microstructural modifications contribute to a more uniform and refined matrix, translating into improved load-bearing capacity and structural integrity of the final component.

This study aims to identify the optimal parameters for incorporating MWCNTs and Al<sub>2</sub>O<sub>3</sub> using EMS to achieve a more uniform microstructure distribution and maximize the composite's mechanical properties. Microstructural characterization and tensile testing were conducted to determine the mechanical properties of the heat-treated samples.

## 2. MATERIALS AND METHODS

### 2.1 Taguchi Method

The Taguchi method was implemented in Minitab software to design the experiment and analyze the results. Table 1 shows the three parameters involved in this experiment with two different levels. The selection of Taguchi levels for MWCNTs content, Al<sub>2</sub>O<sub>3</sub> content and stirring time in the fabrication of metal matrix composites (MMCs) using electromagnetic stirring (EMS) is grounded in recent experimental research and process feasibility. For MWCNTs, weight percentages of 0.5% and 1.0% were chosen based on prior studies demonstrating that low concentrations in this range lead to significant improvements in mechanical properties, such as hardness, tensile strength and wear resistance, without causing agglomeration. For example, Feijoo et al. [9] reported that 0.5 wt.% MWCNTs provided an optimal balance between strength and ductility in AA7075-based composites, while Sharma et al. [10] demonstrated that 1.0 wt.% MWCNTs significantly improved wear resistance and compressive strength, with maximum wear resistance achieved at 0.5 wt.% MWCNTs due to optimal dispersion.

**Table 1:** Condition parameters

Parameter	Level 1	Level 2
MWCNTs Content (wt.%)	0.5	1.0
Al <sub>2</sub> O <sub>3</sub> Content (wt.%)	4.0	6.0
Stirring Time (min)	5.0	10.0

For Al<sub>2</sub>O<sub>3</sub>, levels of 4 wt.% and 6 wt.% are consistent with established ranges used in MMC fabrication, providing improved hardness and wear resistance while avoiding excessive brittleness and porosity that can occur at higher concentrations. These levels are widely used in both academic studies and industry [7]. As for stirring time, Wakhi Anuar et al. [11] demonstrated that a 5-minute stirring duration was sufficient to achieve uniform dispersion of reinforcements within the molten matrix. However, with increased reinforcement content, a longer stirring time is necessary to prevent clustering and agglomeration. Therefore, a 10-minute stirring duration was selected to ensure effective distribution.

By setting up an orthogonal array, Minitab allows for efficient testing of all possible combinations of these parameters with minimal experimental runs, as tabulated in Table 2. Each parameter is assigned to two levels, which represent the different conditions under which they are tested. This systematic approach not only saves time and resources but also helps in identifying the specific combination of MWCNTs content, Al<sub>2</sub>O<sub>3</sub> content and stirring time that leads to the best material properties.

**Table 2:** L8 Orthogonal array

No. of Run	MWCNTs Content (wt.%)	Al <sub>2</sub> O <sub>3</sub> Content (wt.%)	Stirring Time (min)
1	0.5	4	5
2	0.5	4	10
3	0.5	6	5
4	0.5	6	10
5	1.0	4	5
6	1.0	4	10
7	1.0	6	5
8	1.0	6	10

**2.2 Experimental Procedure**

The fabrication process of the matrix is illustrated in Figure 1. The alloy used in this process is a commercially-available A356 aluminium alloy, provided in ingot form. Its chemical composition, determined via spectrometry and expressed in weight percentages, includes 7.38% silicon (Si), 0.26% magnesium (Mg), 0.0463% copper (Cu), 0.25% iron (Fe), 0.190% manganese (Mn), 0.0068% zinc (Zn) and 0.0411% titanium (Ti). First, the particle size of Al<sub>2</sub>O<sub>3</sub> was reduced to improve interfacial bonding and decrease particle pull-out under stress. The planetary ball-milling process was performed for 12 hours at 200 rpm using an alumina jar and alumina balls with a ball-to-powder ratio of 5:1. To prevent overheating, a milling cycle with 5-minute intervals was applied after every 15 minutes of operation. The particle size was successfully reduced from 63 μm to 30.2 μm, as confirmed by a particle size analyzer (Malvern Mastersizer Hydro 2000MU & Scirocco 2000 Particle Analyser). The effective size of the alumina in the metal matrix composite ranges from 8 μm to 53 μm. The study by Murthy et al. [12] demonstrated the effect of the particle size of Al<sub>2</sub>O<sub>3</sub> on hardness. This work investigated Al<sub>2</sub>O<sub>3</sub> particles between three different sizes of 20 μm, 53 μm and 88 μm and the smallest one shown to have highest hardness.

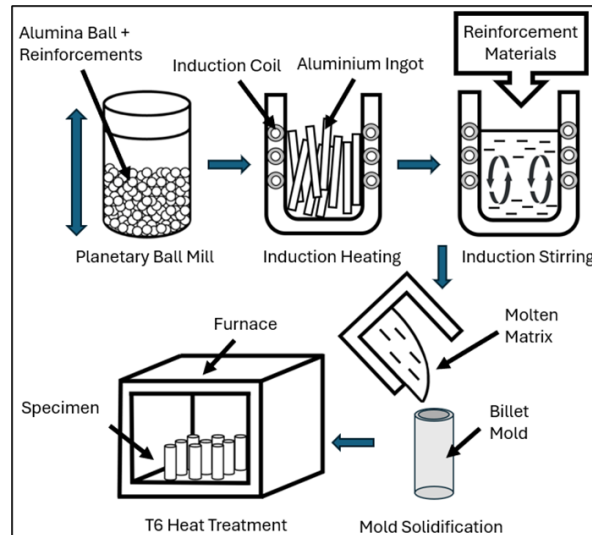


**Figure 1:** Fabrication process of MMCs

The inclusion of magnesium powder serves as an effective strategy to enhance wettability by reducing the contact angle between the liquid and solid phases [13]. Then, to remove moisture, the magnesium powder, alumina, and multiwall carbon nanotubes were mixed well, wrapped in aluminium foil, and subjected to preheating at about 200 °C. The induction furnace heats the aluminium ingot to 750 °C; then, the temperature is lowered to 710 °C and held for 20 minutes to ensure thermal stability and reduce temperature fluctuations. Stabilizing the molten metal at this stage is crucial for minimizing gas porosity and improving casting quality. Following this period, the temperature is further reduced to 660 °C, an optimal range for adding reinforcements without causing significant cooling or premature

solidification. At 660 °C, preheated reinforcement materials are gradually introduced into the molten aluminium, with electromagnetic stirring applied to ensure uniform distribution within the matrix. The induction furnace operates at 400 V, 15 kW, 100 A, and a frequency of 2.2 kHz, creating an alternating electromagnetic field that induces eddy currents, promoting uniform stirring of the molten alloy.

After the casting process, the billet underwent material characterization. The Al-MMCs were characterized by utilizing several testing and analysis techniques, including optical microscopy, X-ray diffraction (XRD), and mechanical testing. The microstructure distribution of Al<sub>2</sub>O<sub>3</sub>-CNTs in the composites was examined using a Nikon Optical Microscope and Field Emission Scanning Electron Microscopy (ZEISS Sigma 500, Germany). The microstructure analysis was conducted after grinding the samples with different grit sizes (400, 600, 800 and 1200) and polished with diamond paste until achieving a mirror-like surface. The samples were etched with Keller's reagent (2.5 ml HNO<sub>3</sub>, 1.5 ml HCl, 1 ml HF, 95 ml distilled water) for 10-12 seconds, rinsed with distilled water, and dried using a rubber bulb air blower to prevent watermark formation. Tensile tests were performed using a 100 kN universal testing machine at 5 mm/sec speed. The samples were fabricated into a dog-bone shape according to the ASTM E8M standard for each group, as depicted in Figure 2. Three samples were utilized in this experiment to provide reliable data analysis.

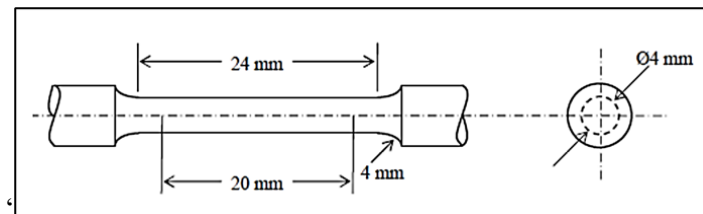


Figure 2: Dog bone specimen based on ASTM E8M [14]

### 3. RESULTS AND DISCUSSION

#### 3.1 Microstructural characterization

Figure 3 illustrates the microstructural evolution of Al<sub>2</sub>O<sub>3</sub>-CNTs-reinforced A356 matrix composite after electromagnetic stirring and T6 heat treatment. The microstructure of the composite in Figure 3(a) shows the primary  $\alpha$ -Al phase appearing in rosette-like and nearly globular morphologies, with silicon exhibiting a plate-like form typical of the dendritic structure in as-cast alloys. According to Wakhi Anuar et al. [14], the structural transformation results from vortex mechanical forces, where external forces break the dendritic arms and lead to isolated structures. The integration of Al<sub>2</sub>O<sub>3</sub>-CNTs into an aluminium matrix significantly enhances the microstructural refinement of aluminium composites. This improvement is largely attributed to heterogeneous nucleation within the aluminium melt. In metal composites, heterogeneous nucleation occurs when added particles act as sites for crystal formation, allowing the material to form a finer, more uniform structure [15]. When Al<sub>2</sub>O<sub>3</sub>-CNTs particles enter the aluminium melt, they serve as crucial nucleation sites, enabling the development of a refined composite microstructure. During solidification, reinforcement particles of Al<sub>2</sub>O<sub>3</sub>-CNTs concentrate in specific regions of the aluminium matrix, particularly in the eutectic-silicon (Si) areas. These regions are critical to the composite's strength and durability, as they directly impact the arrangement and cohesion of the grains. By concentrating in the eutectic-Si regions, the reinforcement particles remain immobilized, shaping the  $\alpha$ -Al phases, which helps produce a more consistent and closely packed grain structure within the material. This process yields a composite material with a highly refined grain structure, characterized by smaller, well-packed grains that are expected to enhance the mechanical properties of the composite [16].

The microstructures of T6 heat-treated samples in Figure 3(b) exhibit further coarsening of  $\alpha$ -Al globules compared to Figure 3(a). The plate-like eutectic-Si particles have largely transformed into a rounded shape and are embedded between the  $\alpha$ -Al globules. The T6 heat treatment alters the eutectic-

Si morphology during solution treatment, creating an inter-granular contrast during artificial aging. At the start of the heating process or at low liquid fractions, coalescence occurs between adjacent  $\alpha$ -Al grains. Ostwald ripening also takes place, as smaller  $\alpha$ -Al globules with high interfacial energy merge into larger globules to reduce energy. Both coalescence and Ostwald ripening contribute to the coarsening of  $\alpha$ -Al globules [17].

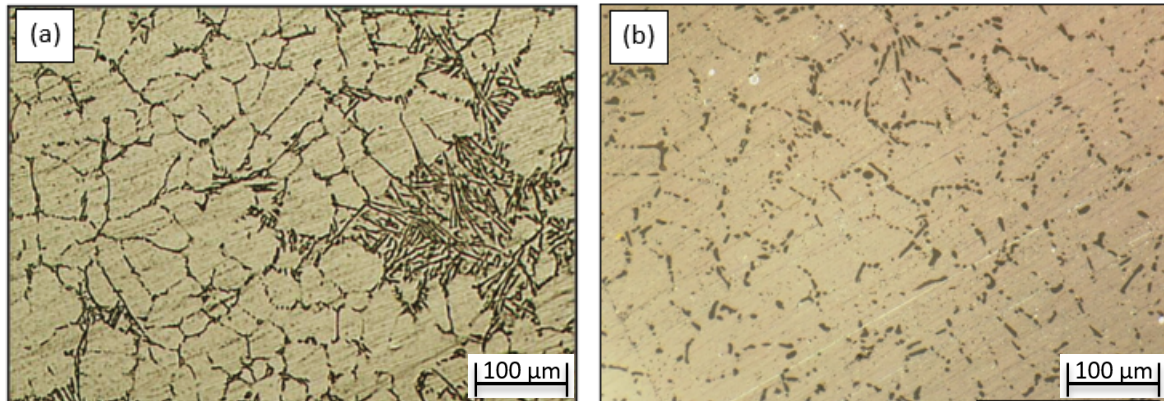


**Figure 3:** OM Result for sample 4 (0.5 wt.% CNTs, 6 wt.% Al<sub>2</sub>O<sub>3</sub>, 10-minute stirring): (a) Before T6 and (b) After T6

### 3.2. Field Emission Microscopy

All Figure 4 shows FESEM images taken before and after T6 heat treatment, revealing irregularly shaped intermetallic particles dispersed within the aluminium matrix. Based on the XRD results, these intermetallic phases likely include Al<sub>2</sub>Cu, Mg<sub>2</sub>Si, Al<sub>4</sub>C<sub>3</sub> and possibly Al<sub>8</sub>Fe<sub>2</sub>Si. The coarse morphology of these phases indicates that they are primarily in an unrefined state, as they have not undergone the dissolution and re-precipitation that occurs during T6 heat treatment. The visible needle-like or platelet structures are characteristic of Mg<sub>2</sub>Si and Al<sub>2</sub>Cu phases. The Al<sub>4</sub>C<sub>3</sub> particles, formed from the reaction of aluminium with carbon from the CNTs, may also contribute to this morphology. Additionally, iron-containing phases like Al<sub>8</sub>Fe<sub>2</sub>Si can be observed in irregular, sometimes elongated shapes, which can act as brittle inclusions and may adversely affect the material's ductility. Fe content in the composite must be kept below 0.7% to prevent sticking in die-casting moulds. Exceeding this limit can adversely affect the alloy's mechanical properties, which degrade the composite's hardness [18]. However, through heat treatment, the morphology of intermetallic phases can be altered, as needle-like or plate-like phases transform into more spherical or globular forms, as illustrated in Figure 4(b). This transformation is beneficial, as spherical intermetallic often reduces stress concentration points and improve the composite's toughness.

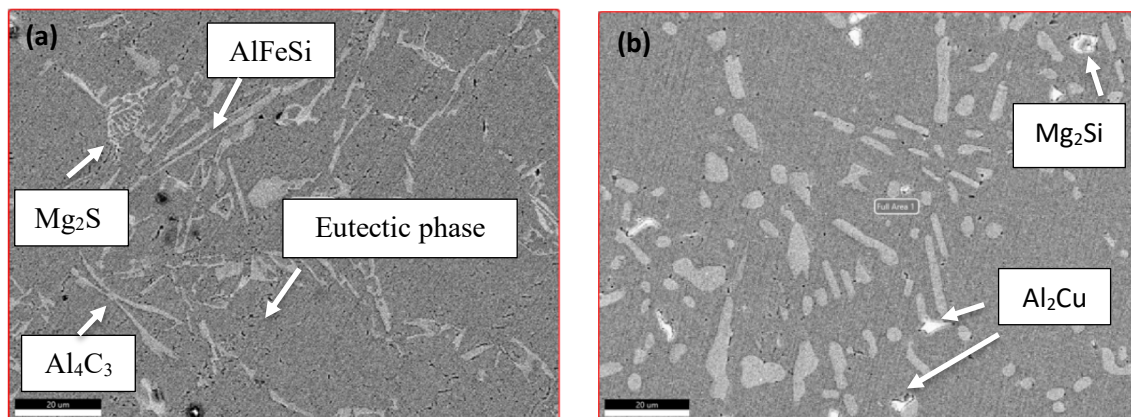


**Figure 4:** FESEM Result for sample 4 (0.5 wt.% CNTs, 6 wt.% Al<sub>2</sub>O<sub>3</sub>, 10 minutes stirring): (a) before T6 and (b) after T6

The X-ray diffraction (XRD) analysis of the aluminium composite, reinforced with MWCNTs- $\text{Al}_2\text{O}_3$  and produced via electromagnetic casting, reveals significant changes in phase intensity, indicating microstructural evolution, as shown in Figure 5. Before heat treatment, the diffraction peaks of aluminium (Al), which exhibits a face-centered cubic (FCC) structure, are clearly observed with characteristic reflections at  $\{111\}$ ,  $\{200\}$ , and  $\{220\}$ , as the main composition in the matrix. The incorporation of CNTs is evidenced by a carbon peak at  $44^\circ$   $\{200\}$  and  $78^\circ$   $\{311\}$ . Additionally, peaks corresponding to  $\text{Al}_2\text{O}_3$  indicate the uniform distribution of alumina particles within the aluminium matrix, with distinct peaks appearing at  $38^\circ$   $\{111\}$ . The other intermetallic phases found were  $\text{Mg}_2\text{Si}$  at  $38^\circ$   $\{111\}$  and  $44^\circ$   $\{200\}$ , and  $\text{Al}_4\text{C}_3$  at  $38^\circ$   $\{111\}$ . The presence of reinforcement phases such as  $\text{Al}_2\text{O}_3$  and carbon, along with intermetallic compounds like  $\text{Al}_2\text{Cu}$ ,  $\text{Al}_8\text{FeSi}$ , and  $\text{Mg}_2\text{Si}$ , are also observed, albeit with relatively low intensities. This suggests a less developed crystalline structure and minimal precipitation of strengthening phases.

After T6 heat treatment, the intensity of the aluminium peaks, especially the  $\{200\}$  and  $\{220\}$  reflections, increases substantially, indicating improved crystallinity and possible grain refinement. Notably, the peaks associated with  $\text{Al}_2\text{Cu}$  and  $\text{Mg}_2\text{Si}$  become more prominent, confirming the precipitation and growth of these hardening phases during the artificial aging stage of the T6 process. This transformation enhances the material's mechanical properties by contributing to strengthening mechanisms. Meanwhile, the peaks for  $\text{Al}_4\text{C}_3$  and carbon remain relatively unchanged, suggesting that these phases are thermally stable under the applied heat treatment conditions. Overall, the XRD results demonstrate that T6 heat treatment promotes the nucleation and crystallization of intermetallic phases, leading to a more refined and reinforced microstructure within the aluminium matrix composites. The distribution of MWCNT and  $\text{Al}_2\text{O}_3$  in electromagnetic stirring had achieved uniform dispersion of the reinforcements within the matrix.

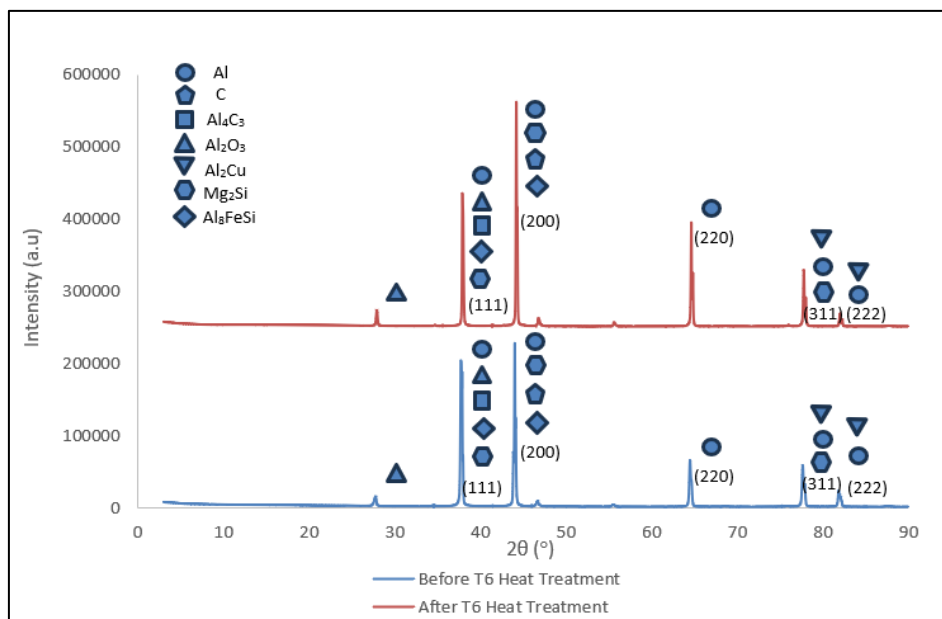


**Figure 5:** XRD Result of matrix composite before and after T6 heat treatment

### 3.3. Mechanical Testing

The mechanical properties of aluminium matrix composites reinforced with  $\text{Al}_2\text{O}_3$ -CNTs, as tabulated in Table 3 and Figure 6, offer important insights into how variations in composition and stirring time affect key characteristics, such as yield strength, ultimate tensile strength, elongation at fracture and hardness. Sample 4 stands out as the most effective matrix composite, showcasing the highest mechanical properties, with an optimal yield strength of 94.09 MPa, ultimate tensile strength of 221.10 MPa and elongation at fracture of 11.37%. Subsequently, after the T6 heat treatment, the

mechanical strength of all samples increased significantly, as tabulated in Table 4 and Figure 7. Sample 4 exhibited increases in yield strength, ultimate tensile strength, and elongation to fracture to 117.18 MPa, 288.08 MPa and 14.5%, respectively. This performance suggests that a combination of 0.5 wt.% MWCNT, 6 wt.% Al<sub>2</sub>O<sub>3</sub> and a stirring time of 10 minutes yields the best mechanical outcomes. In contrast, Sample 1, which demonstrates the lowest values for strength and ultimate tensile strength (UTS), highlights the adverse effects of insufficient stirring time (5 minutes) on both strength and reinforcement distribution.

The data revealed an inverse relationship between the content of CNTs and Al<sub>2</sub>O<sub>3</sub> in the matrix. For example, samples containing 0.5 wt.% CNTs (Samples 1, 2, 3 and 4) exhibited higher mechanical strength compared to samples with 1.0 wt.% CNTs (Samples 5, 6, 7 and 8). The results indicate that increasing CNT content beyond 0.5 wt.% does not significantly enhance composite strength and leads to agglomeration, which weakens the interfacial bonding and compromises overall material performance. Percolation theory suggests that there exists an optimal concentration of carbon nanotubes (CNTs) to achieve effective dispersion within the matrix. If this concentration is exceeded, excessive clustering occurs, diminishing the composite's reinforcement capacity. Here, the optimal CNT concentration is determined to be 0.5 wt.%, and any increase beyond this threshold risks degrading the matrix composite's properties [19]. In contrast, matrix composites with a higher Al<sub>2</sub>O<sub>3</sub> content of 6 wt.% (Samples 3, 4, 7, and 8) displayed better tensile results than those with 4 wt.% Al<sub>2</sub>O<sub>3</sub> content (Samples 1, 2, 5, and 6). This shows the importance of reducing the size of Al<sub>2</sub>O<sub>3</sub> in terms of maximizing the uniform distribution throughout the matrix. In fact, smaller alumina particles have a larger surface-area-to-volume ratio, which enhances their bonding with the matrix material [20]. This improved interface contributes to better load transfer across the composite, thereby strengthening the overall material.

Stirring duration emerges as a crucial factor in optimizing the mechanical properties of the matrix. The results indicate that a stirring time of 10 minutes is sufficient to facilitate the wetting of reinforcement particles within the molten metal. Effective wettability ensures that the particles are thoroughly coated by the matrix, thus enhancing load transfer and improving composite strength. Additionally, an optimized stirring duration helps to break down and evenly distribute grains throughout the matrix, further contributing to increased hardness and mechanical strength.

**Table 3:** Mechanical properties before T6 heat treatment

Sample	Yield Strength (MPa)	Ultimate Tensile Strength (MPa)	Elongation to Fracture (%)
1	74.77	170.37	9.33
2	84.16	206.25	10.32
3	82.45	204.82	9.23
4	94.09	221.10	11.37
5	76.05	201.40	8.96
6	93.79	209.88	9.34
7	86.81	211.74	9.47
8	88.99	211.70	10.31

**Table 4:** Mechanical properties after T6 heat treatment

Sample	Yield Strength (MPa)	Ultimate Tensile Strength (MPa)	Elongation to Fracture (%)
1	82.43	212.59	11.24
2	92.48	236.55	13.11
3	89.92	225.12	12.25
4	117.18	288.08	14.56
5	89.63	261.63	11.29
6	105.85	268.99	12.14
7	109.71	273.30	12.30
8	114.10	276.89	13.17

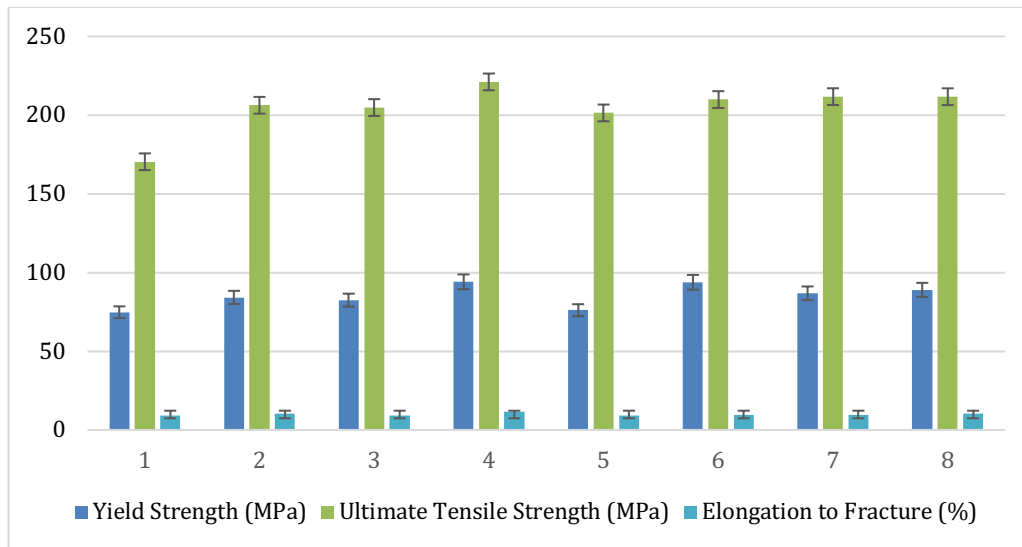


**Figure 6:** Mechanical properties of the composite before T6.

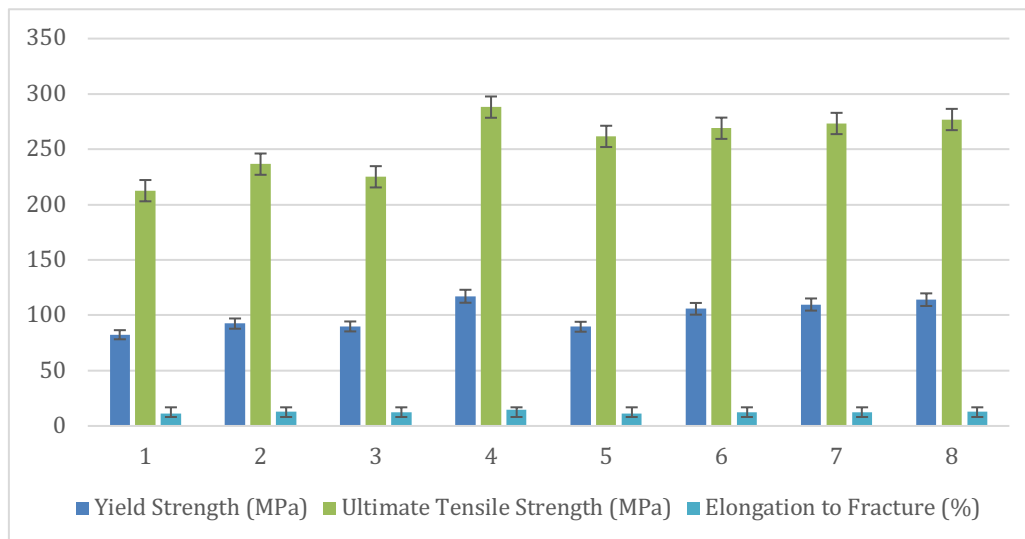


**Figure 7:** Mechanical properties of the composite after T6.

#### 4. CONCLUSIONS

The integration of Al<sub>2</sub>O<sub>3</sub>-CNTs into A356 aluminium was successfully achieved through EMS casting. Among the specimens tested, specimen 4, containing 0.5 wt.% CNTs, 6 wt.% Al<sub>2</sub>O<sub>3</sub> and stirred for 10 minutes, stood out, demonstrating the highest performance. After T6 heat treatment, its mechanical strength improved significantly, with yield strength increasing from 72.38 MPa to 90.14 MPa, ultimate tensile strength from 170.08 MPa to 221.6 MPa and elongation to fracture from 11.37% to 14.5%. The compressive strength of hybrid metal matrix composites (MMCs) also increased with higher Al<sub>2</sub>O<sub>3</sub> content compared to the A356 alloy. However, the relationship between CNT content and strength is nonlinear; excessive Al<sub>2</sub>O<sub>3</sub> or CNTs may negatively affect material properties due to issues like agglomeration or poor wettability with the matrix. The heat treatment promotes the formation of intermetallic compound precipitates, which strengthens the matrix by hindering dislocation motion. Additionally, heat treatment can refine the grain structure, enhancing strength due to the Hall-Petch relationship, where smaller grain sizes lead to increased mechanical properties of the composite. A potential direction for future research involves increasing the CNT loading by employing ultrasonic-assisted electromagnetic stirring. This hybrid technique introduces high-frequency ultrasonic waves

into the molten metal, generating cavitation bubbles that collapse with high energy, effectively breaking apart CNT agglomerates and promoting more uniform and stable dispersion throughout the matrix.

### Acknowledgements

The study is funded by the Ministry of Higher Education (MOHE) of Malaysia through the Fundamental Research Grant Scheme (FRGS), No. FRGS/1/2022/TK10/UTEM/02/18. The authors would also like to thank Universiti Teknikal Malaysia Melaka (UTeM) for supporting this study.

### Author Contributions

All authors contributed toward data analysis, drafting and critically revising the paper and agree to be accountable for all aspects of the work.

### Disclosure of Conflict of Interest

The authors have no disclosures to declare.

### Compliance with Ethical Standards

The work is compliant with ethical standards.

### References

- [1] Xavier, J. R. & Vinodhini, S. P. (2024). Advanced nanocomposite coating for aluminium alloy with enhanced corrosion resistance, flame retardancy, and mechanical strength in aircraft manufacturing industries. *Colloids and Surfaces A: Physicochemical and Engineering Aspects*, 698, 134543.
- [2] Zhang, W. & Xu, J. (2022). Advanced lightweight materials for Automobiles: A review. *Materials & Design*, 221, 110994.
- [3] Haque, S., Rahman, M. A., Shaikh, R. R., Sirajudeen, N., Kamaludeen, M. B. & Sahu, O. (2022). Effect of powder metallurgy process parameters on tribology and micro hardness of Al6063-nano Al<sub>2</sub>O<sub>3</sub> MMCs. *Materials Today: Proceedings*, 68, 1030-1037.
- [4] Rajendran, C. & Saiyathibrahim, A. (2024). Influence of B<sub>4</sub>C and ZrB<sub>2</sub> reinforcements on microstructural, mechanical and wear behaviour of AA 2014 aluminium matrix hybrid composites. *Defence Technology*, 40, 242-254.
- [5] Srinivasan, R., Hariharan, K., Jeyanthan, S. A., Kamalesh, M. & Ali, I. (2022). Effect of addition of titanium carbide and graphite reinforcement on Al7075 hybrid metal matrix composites by gravity stir casting method. *Materials Today: Proceedings*, 62, 86-93.
- [6] Sadeghi, B. & Cavaliere, P. (2022). CNTs reinforced Al-based composites produced via modified flake powder metallurgy. *Journal of Materials Science*, 57(4), 2550-2566.
- [7] Shan, Y., Pu, B., Liu, E., Shi, C., He, C. & Zhao, N. (2020). In-situ synthesis of CNTs@ Al<sub>2</sub>O<sub>3</sub> wrapped structure in aluminum matrix composites with balanced strength and toughness. *Materials Science and Engineering: A*, 797, 140058.

- [8] Sharma, O., Gupta, P. & Kumar, T. (2022). Fabrication and characterisation of aa6063-t6/sic/waste bone powder using electromagnetic stir casting. In *IOP Conference Series: Materials Science and Engineering*, 1248 (1), 012076.
- [9] Feijoo, I., Pena, G., Cabeza, M., Cristóbal, M. J. & Rey, P. (2021). MWCNT-reinforced AA7075 composites: effect of reinforcement percentage on mechanical properties. *Metals*, 11(6), 969.
- [10] Sharma, R., Sasikumar, C. & Baral, J. (2024). Wear behaviour of Al-MWCNT composites by varying MWCNTs concentration. *Journal of Alloys and Metallurgical Systems*, 7, 100104.
- [11] Anuar, N. F. B. W., Omar, M. Z., Salleh, M. S., Zamri, W. F. H. W. & Ali, A. M. (2024). Effect of graphene addition on microstructure and wear behaviour of the A356-based composite fabricated by thixoforming process. *Journal of Materials Research and Technology*, 30, 4813-4831.
- [12] Murthy, B. V., Auradi, V., Nagaral, M., Vatnalmath, M., Namdev, N., Anjinappa, C. & Qamar, M. O. (2023). Al2014–alumina aerospace composites: particle size impacts on microstructure, mechanical, fractography, and wear characteristics. *ACS omega*, 8(14), 13444-13455.
- [13] Malaki, M., Fadaei Tehrani, A., Niroumand, B. & Gupta, M. (2021). Wettability in metal matrix composites. *Metals*, 11(7), 1034.
- [14] Anuar, N. F. B. W., Omar, M. Z., Salleh, M. S. & Hakim, W. F. (2024). Effect of short heat treatments on the microstructural evolution and hardness of thixoformed graphene reinforced aluminium composites. *Sains Malaysiana*, 53(3), 705-717.
- [15] Balasubramani, N., Venezuela, J., StJohn, D., Wang, G. & Dargusch, M. (2023). A review of the origin of equiaxed grains during solidification under mechanical stirring, vibration, electromagnetic, electric-current, and ultrasonic treatments. *Journal of Materials Science & Technology*, 144, 243-265.
- [16] Na'aim Abd Rahim, M., Salleh, M. S., Subramonian, S., Kamal, M. R. M. & Al-Zubaidi, S. S. (2023). Influence of graphene on the microstructure and mechanical properties of aluminium matrix composite. *Malaysian Journal on Composites Science and Manufacturing*, 12(1), 73-83.
- [17] Zhang, Y., Jiang, J., Wang, Y., Liu, Y. & Huang, M. (2022). Microstructural evolution and anisotropic tensile properties of a bimodal 6A02 Al semi-solid billet. *Journal of Alloys and Compounds*, 910, 164937.
- [18] Luo, A. A., Sachdev, A. K. & Apelian, D. (2022). Alloy development and process innovations for light metals casting. *Journal of Materials Processing Technology*, 306, 117606.
- [19] Sarkar, L., Saha, S., Samanta, R., Sinha, A., Mandal, G., Biswas, A. & Das, A. (2024). Recent progress in CNT-reinforced composite and FGM for multi-functional space applications and future directions. *Journal of The Institution of Engineers (India): Series D*, 105(1), 527-541.
- [20] Luo, H., Li, J., Guan, B., Ye, J., Wang, Y., Chen, X. & Pan, F. (2024). Investigating the microstructure-property relationship in Mg matrix composites reinforced by particles of different sizes using experiments combined with finite element simulation. *Powder Technology*, 433, 119220.